Dynamics and Optimization of Rifle Barrel Vibrations

From ballistic theory to finite-element simulation

Contents

1 Introduction: principles of positive compensation

This first section presents the *why* and the *how* of positive compensation without resorting to mathematical tools. A curious reader who only wishes to understand the idea and its practical interest may stop at the end of section 1.8; the subsequent sections then develop the rigorous modelling and the numerical simulation.

1.1 The challenge of precision shooting

In precision-shooting disciplines (for instance, ISSF 50-metre prone), the pursuit of a perfect group runs up against the physical limits of the ammunition. Even with *match*-grade cartridges, there remains an unavoidable variation in muzzle exit velocity — the *muzzle velocity* — from one cartridge to the next. This variation, often measured in feet per second (fps), is typically on the order of a few percent.

1.2 Why a variation in velocity moves the point of impact

A slower bullet spends more time in flight to reach the target and therefore suffers gravitational acceleration for longer: it drops more. Mechanically, on target, this translates into a lower impact than a faster bullet fired with the same setting. If the barrel were a perfectly rigid and stationary tube, the velocity spread of the cartridges would inevitably translate into a *vertical streak* on the target: fast bullets at the top, slow ones at the bottom.

1.3 The barrel vibrates like a tuning fork

In reality, when the shot is fired, the barrel does not stay still: it begins to vibrate. The powder explosion, the recoil of the firearm, the projectile's travel through the bore and its friction against the rifling all excite transverse oscillations — that is, up-and-down and side-to-side — that move the muzzle by a few hundredths of a degree, in the manner of a tuning fork ringing after being struck. These vibrations last several tens of milliseconds, well beyond the time it takes for the bullet to travel through the barrel (typically 2 to 3 milliseconds).

During those 2 to 3 milliseconds, the muzzle is therefore in motion: it rises, falls, returns through its equilibrium position, and so on. The exact angle at which the bullet exits depends not only on the shooter's aim, but also on the *precise instant* of exit.

1.4 What sets the magnitude of the vibrations

Where does this motion come from? The dominant source, emphasised by G. Kolbe [7], is *recoil*: under the thrust of the gases, the whole firearm moves backwards and *rotates about its centre of gravity*. The barrel axis (the bore line, through which the bullet exits) lies *above* that centre of gravity; the recoil thrust therefore acts with a *lever arm* and imparts a couple to the rear of the barrel, exactly as a flick delivered off-centre tips a ruler lying on a table. This couple is the "hammer blow" that makes the tuning fork ring.

Two concrete quantities then govern the *amplitude* of the muzzle motion:

- the **total weight of the firearm**: a heavy rifle absorbs recoil while moving less, and therefore vibrates less;

- the **height of the bore above the centre of gravity**: the larger this lever arm, the larger the couple — and hence the amplitude.

Neither parameter appears in the tuner setting (which acts on the *rhythm* of the vibrations, not on their cause), but together they explain why two rifles with identical barrels but different mountings do not tune the same way. They are reintroduced formally in Section 3.4 as the excitation moment $M_0(t)$.

1.5 The principle of positive compensation

The brilliant idea, proposed as early as 1901 by A. Mallock [8] and formalised for modern shooting by G. Kolbe (Border Barrels) [5, 6], is to *exploit* these vibrations rather than suffer them. If one manages to tune the barrel so that the muzzle is *rising* at the precise moment the bullet leaves it, then:

- a **fast** bullet exits slightly *early*: at that moment, the barrel has not yet had time to rise much, and the bullet is launched at a *lower* angle (figure 1, red trajectory);
- a **slow** bullet exits slightly *late*: the barrel has continued to rise, and the bullet is launched at a *higher* angle (blue trajectory).

The slow bullet is therefore projected *higher* initially; on target, its extra drop (because it spent longer in flight) is exactly compensated by its extra starting height. All bullets, fast or slow, can thus end up at the *same* point of impact. This is what Kolbe calls *positive compensation*.

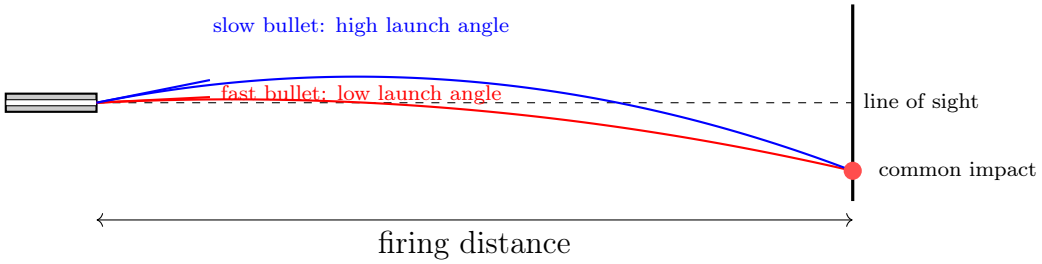

Figure 1: Geometric principle of positive compensation. If the muzzle is rising when the bullets exit, the slower bullets (which leave later) benefit from a higher launch angle. Their extra starting height compensates the extra drop due to their longer flight, and all bullets can end up at the same point of impact on target.

1.6 The role of the tuner

For this phenomenon to occur, one still needs to *match* the barrel's vibrations to the bullet's exit time — hence the term *tuner*, which denotes a movable mass (typically 100 to 400 grams) fixed to the muzzle of the barrel. By screwing this mass in or out, the shooter moves it closer to or farther from the muzzle, which subtly modifies the barrel's vibration frequency. This amounts to adjusting the rhythm of the "tuning fork": one lengthens or shortens the time it takes for the muzzle to return through its equilibrium position, so that this instant falls precisely when the average bullet exits.

Any change of ammunition or even of lot in principle requires a new adjustment, since the average velocity — and therefore the barrel travel time — changes. Shooters typically proceed by successive trials (the so-called *ladder* or *Audette* method [9]): one fires several series while changing the tuner position by one notch each time, and retains the position for which the groups are tightest.

1.7 Intuitive summary

In summary, positive compensation requires three ingredients:

1. a barrel that vibrates enough to move noticeably between the exit of a fast bullet and that of a slow bullet;
2. a *tuning* of these vibrations that places the exit time of the average bullet at the right point of the oscillation (the *rising* phase);
3. a quantitative compromise between the angular speed of the motion and the ballistic drop: a barrel that rises too slowly will not compensate enough for the dispersion, and a barrel that rises too fast will over-compensate.

The following sections formalise each of these three ingredients and show how the physical parameters of the barrel, the tuner and the ammunition combine to reach the optimum.

1.8 Document outline

The remainder of the document develops the theory and the simulation:

- Section 2: list of notations and conventions used.
- Section 3: mathematical modelling of the barrel (Euler-Bernoulli beam, finite-element method, Newmark-β time integration).
- Section 4: analysis of natural frequencies and sensitivity to the tuner.
- Section 5: mathematical criterion of positive compensation, distinction between temporal node and antinode, experimental confirmation by Kolbe, and validation by the numerical simulation.
- Section 6: practical conclusions for the shooter.

2 Notations and conventions

We adopt the SI system of units $(\mathrm{m}, \mathrm{kg}, \mathrm{s}, \mathrm{Pa}, \mathrm{rad})$. The x-axis is aligned with the bore of the barrel, oriented from the breech ($x = 0$) toward the muzzle ($x = L$). The y-axis is transverse, oriented upward. Unless otherwise stated, angles are in radians; the usual conversions are 1 MOA $= \pi/(180 \times 60)$ rad $\approx 2.909 \times 10^{-4}$ rad and 1 mrad ≈ 3.438 MOA.

Symbol	Meaning	Unit
Barrel geometry and material		
L	Barrel length	m
$D_{\text{ext}}, D_{\text{int}}$	Outer (profile) and inner (bore) diameters	m
A	Cross-sectional area $\frac{\pi}{4}(D_{\text{ext}}^2 - D_{\text{int}}^2)$	m^2
I	Second moment of area $\frac{\pi}{64}(D_{\text{ext}}^4 - D_{\text{int}}^4)$	m^4
E	Young's modulus (steel ≈ 200 GPa)	Pa
ρ	Mass density (steel ≈ 7850 kg/m^3)	kg/m^3
EI	Flexural rigidity	$\text{N}\cdot\text{m}^2$
ρA	Mass per unit length	kg/m
Beam kinematics		
$y(x,t)$	Transverse deflection at point x and time t	m
$\theta(x,t) \equiv \partial y/\partial x$	Slope / angle of the neutral axis	rad
$\theta(L,t)$	Angle at the muzzle (launch angle)	rad
$\dot{\theta} = \partial\theta/\partial t$	Muzzle angular velocity	rad/s
Tuner		
m_t	Tuner mass (typically 100–400 g)	kg
J_t	Tuner transverse moment of inertia	$\text{kg}\cdot\text{m}^2$
Natural modes		
ω_n	Angular natural frequency of mode n	rad/s
$f_n = \omega_n/(2\pi)$	Natural frequency of mode n	Hz
$T_n = 1/f_n$	Natural period of mode n	s
$\phi_n(x)$	Spatial shape of mode n	—
ζ_n	Modal damping ratio	—
Projectile and internal ballistics		
m_p	Projectile mass (.22 LR: ≈ 2.6 g)	kg
$v(x,t)$	Projectile velocity at position x	m/s
v_0, v_{muzzle}	Muzzle velocity (at exit)	m/s
$\bar{v}$	Effective average velocity in the barrel	m/s
t_b	Projectile travel time in the barrel	s
$p(t)$	Pressure in the chamber / bore	Pa
$A_{\text{bore}} = \frac{\pi}{4}D_{\text{int}}^2$	Effective cross-sectional area of the bore	m^2
$\tau_v \equiv -\partial t_b/\partial v_0$	Sensitivity of exit time to muzzle velocity	s/(m/s)
Target and compensation		
D	Shooting distance (50 m for ISSF prone)	m
g	Gravitational acceleration (≈ 9.81 m/s^2)	m/s^2
$h_{\text{bal}}(v_0)$	Ballistic drop at distance D	m
θ_{out}	Muzzle angle at instant t_b: $\theta(L, t_b)$	rad
$\dot{\theta}^\star_{\text{out}}$	*Target* angular velocity for full compensation	rad/s
Numerical simulation		
N	Number of finite elements	—
$L_e = L/N$	Element length	m
$[K], [M], [C]$	Global stiffness, mass, damping matrices	—
$\{u(t)\}$	Vector of nodal DOFs (translations + rotations)	—
Δt	Newmark-β time step	s

3 Mathematical development

3.1 Continuous model: Euler–Bernoulli beam

We model the barrel as a prismatic beam clamped at the breech ($x = 0$) and free at the muzzle ($x = L$), with cross-sectional area $A(x)$ and second moment of area $I(x)$ (assumed piecewise constant; *bull*, *sporter* and tapered profiles can be handled by varying these element-wise). Writing $y(x, t)$ for the transverse deflection, the partial differential equation governing small oscillations reads:

$$\rho A \frac{\partial^2 y}{\partial t^2} + \frac{\partial^2}{\partial x^2}\left(EI \frac{\partial^2 y}{\partial x^2} \right) = q(x, t), \tag{1}$$

where $q(x, t)$ represents the distributed transverse load. The boundary conditions are:

$$y(0, t) = 0, \qquad \frac{\partial y}{\partial x}(0, t) = 0, \qquad EI \frac{\partial^2 y}{\partial x^2}\bigg|_{x=L} = M_t, \qquad \frac{\partial}{\partial x}\left(EI \frac{\partial^2 y}{\partial x^2} \right)\bigg|_{x=L} = -F_t,$$

where M_t and F_t respectively denote the moment and the force applied by the tuner (including its inertial effects). For a thick-walled match profile, the Euler–Bernoulli assumption (plane sections remaining plane and normal to the neutral axis) is reasonable as long as $L/D_{\text{ext}} \gtrsim 20$; beyond that, a Timoshenko model accounting for rotational inertia and shear deformation is preferable.

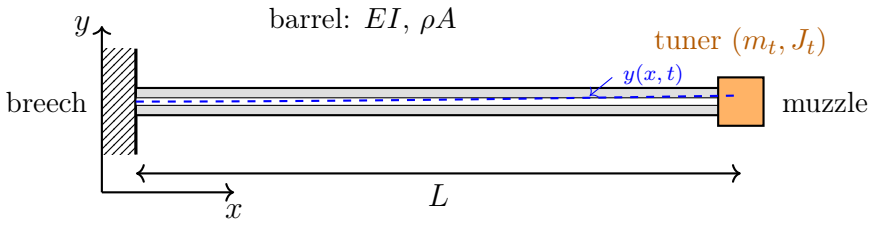

Figure 2: Barrel model: Euler-Bernoulli beam clamped at the breech ($x = 0$), free at the muzzle ($x = L$), carrying at its end a point mass and its rotational inertia (m_t, J_t) representing the tuner. The dashed curve illustrates a transverse deflection $y(x, t)$.

3.2 Finite-element discretisation

We seek a weak solution of (1). Multiplying by a test function $w(x)$ of class $\mathcal{C}^1$ satisfying the essential conditions and integrating by parts twice over $[0, L]$, one obtains the *variational formulation*:

$$\int_0^L \rho A\, \ddot{y}\, w \, \mathrm{d}x + \int_0^L EI\, y'' w'' \, \mathrm{d}x = \int_0^L q\, w \, \mathrm{d}x + [\text{boundary terms}]. \tag{2}$$

The barrel is partitioned into N elements of length L_e. On each element, two degrees of freedom are assigned per node: deflection y and rotation $\theta = y'$. The local field $y_e(\xi)$, where $\xi \in [0, L_e]$ is the local coordinate, is expressed using **cubic Hermite shape functions**:

$$y_e(\xi) = \mathbf{N}(\xi)\, \mathbf{u}_e, \qquad \mathbf{u}_e = \begin{pmatrix} y_1 \\ \theta_1 \\ y_2 \\ \theta_2 \end{pmatrix}, \tag{3}$$

with

$$N_1(\xi) = 1 - 3\bar{\xi}^2 + 2\bar{\xi}^3, \qquad N_2(\xi) = L_e\,(\bar{\xi} - 2\bar{\xi}^2 + \bar{\xi}^3),$$
$$N_3(\xi) = 3\bar{\xi}^2 - 2\bar{\xi}^3, \qquad N_4(\xi) = L_e\,(-\bar{\xi}^2 + \bar{\xi}^3),$$

where $\bar{\xi} = \xi / L_e$. These polynomials guarantee the $\mathcal{C}^1$ continuity at the nodes required by the biharmonic operator of (2).

Substituting (3) into (2), one obtains, for each element, the elementary stiffness matrix

$$[K]^e \;=\; \int_0^{L_e} EI\,(\mathbf{N}'')^\top \mathbf{N}''\,\mathrm{d}\xi \;=\; \frac{EI}{L_e^3}\begin{bmatrix} 12 & 6L_e & -12 & 6L_e \\ 6L_e & 4L_e^2 & -6L_e & 2L_e^2 \\ -12 & -6L_e & 12 & -6L_e \\ 6L_e & 2L_e^2 & -6L_e & 4L_e^2 \end{bmatrix}, \tag{4}$$

and the consistent mass matrix

$$[M]^e \;=\; \int_0^{L_e} \rho A\,\mathbf{N}^\top \mathbf{N}\,\mathrm{d}\xi \;=\; \frac{\rho A L_e}{420}\begin{bmatrix} 156 & 22L_e & 54 & -13L_e \\ 22L_e & 4L_e^2 & 13L_e & -3L_e^2 \\ 54 & 13L_e & 156 & -22L_e \\ -13L_e & -3L_e^2 & -22L_e & 4L_e^2 \end{bmatrix}. \tag{5}$$

The nodal load vector is obtained analogously as $\mathbf{f}_e = \int_0^{L_e} q(\xi,t)\,\mathbf{N}^\top\,\mathrm{d}\xi$.

3.3 Assembly, boundary conditions and tuner integration

The global matrices $[K]$ and $[M]$ of size $2(N+1)\times 2(N+1)$ are assembled by summing the elementary contributions on the shared degrees of freedom. The breech clamping imposes $y(0,t) = 0$ and $\theta(0,t) = 0$: we delete the first two rows and columns of the system, which defines the active sub-matrices $[K]_a$ and $[M]_a$.

Adding the tuner at the muzzle (last node, index $N+1$) translates into adding its mass m_t on the translation degree of freedom and its moment of inertia J_t (computed about the axis perpendicular to the barrel axis, in the vibration plane) on the rotation degree of freedom:

$$[M]_a \;\longleftarrow\; [M]_a \;+\; \underbrace{\begin{bmatrix} \mathbf{0} & & \\ & m_t & 0 \\ & 0 & J_t \end{bmatrix}}_{\text{at the muzzle DOFs}}. \tag{6}$$

If the tuner is modelled as a cylinder of mass m_t, radius R_t and length ℓ_t, its moment of inertia about the transverse axis through its centre of gravity is $J_t = m_t\,(3R_t^2 + \ell_t^2)/12$; an offset d between the tuner's centre of gravity and the muzzle introduces an additional term $m_t d^2$ (parallel-axis theorem) and a mass–rotation coupling $m_t d$ that must be taken into account for a long, offset tuner.

3.4 Modelling of the dynamic excitation

The excitation $\{F(t)\}$ gathers several contributions, heterogeneous in amplitude and spectral bandwidth:

(a) Gas pressure and recoil. The pressure $p(t)$ in the chamber produces a longitudinal force applied at the breech. If the firearm is not held in a perfectly symmetric way (which is always the case), this force induces a transverse moment $M_0(t)$ at the clamped node. We typically model $p(t)$ as a Pierret profile or a Gaussian fit to measured pressure–time curves, with peak amplitude $p_{\max} \sim 200$ MPa for the .22 LR and characteristic duration ~ 0.5 ms.

Physically, this moment is not an artefact of an asymmetric hold: it exists even for an ideally held firearm, because the *bore line is offset from the centre of gravity* of the rifle. Following Kolbe's modelling [7], the free firearm of mass m_r recoils and rotates about its centre of gravity, located a distance h_{cg} *below* the bore line; the recoil force $F_{\mathrm{rec}}(t) = p(t)\, A_{\mathrm{bore}}$ thus acts with this lever arm and imparts to the base of the barrel the moment

$$M_0(t) \;=\; p(t)\, A_{\mathrm{bore}}\, h_{\mathrm{cg}}, \tag{7}$$

while the resulting angular amplitude decreases as $1/m_r$ (a heavy rifle recoils less). The clamped model does not contain the rigid-body recoil motion; we therefore tie the lever arm h_{offset} of Section 5.5 to the physical recoil moment by factoring its dependence,

$$h_{\mathrm{offset}}(m_r, h_{\mathrm{cg}}) \;=\; h_{\mathrm{offset}}^{\mathrm{ref}}\, \frac{h_{\mathrm{cg}}}{h_{\mathrm{cg}}^{\mathrm{ref}}}\, \frac{m_r^{\mathrm{ref}}}{m_r}, \tag{8}$$

where the *single* constant $h_{\mathrm{offset}}^{\mathrm{ref}}$ is calibrated once and for all against the vibration envelope measured by Kolbe for his reference rifle ($m_r^{\mathrm{ref}} = 5$ kg, $h_{\mathrm{cg}}^{\mathrm{ref}} = 25.4$ mm). Rather than recalibrating for each rifle, one then *predicts* the dependence on two quantities measurable on the actual rifle — the total weight m_r (easily weighed) and the bore-to-centre-of-gravity distance h_{cg} (trickier, obtained by balancing): mounting the same barrel on a lighter rifle, or one whose bore sits higher above the centre of gravity, amplifies the vibrations and calls for a fresh tuner setting.

(a′) Boundary conditions: clamping *vs* a compliant action. The model above assumes a perfect clamp at the breech ($y(0) = 0,\ \theta(0) = 0$). This is an idealisation: Kolbe [7] prefers *not* to fix the base and represents the compliance of the receiver by an additional beam segment (~ 100 mm long, ~ 38 mm diameter, ~ 25 mm bore) appended at the rear, the whole assembly recoiling *freely* in space (the *free-recoil* assumption, well approximated by bag shooting but violated if a light rifle is firmly shouldered). Our rigid clamp therefore slightly overestimates the fundamental frequency and ignores the rigid-body recoil motion; it nonetheless remains relevant for the *relative* muzzle angle $\theta(L, t)$, the only quantity that drives compensation (cf. Section 5), and it simplifies the modal analysis. The "compliant action" refinement is the natural extension for quantitative work on a real rifle.

(b) Moving projectile load (weight effect). The projectile, of mass m_p, applies at its current position $x_p(t)$ a transverse force due to gravity (its weight) and to the engagement with the rifling. To first approximation, the projectile is treated as a moving point force:

$$q_p(x, t) \;=\; -m_p\, g\, \delta(x - x_p(t)), \tag{9}$$

where g is the gravitational acceleration and δ the Dirac distribution. The corresponding nodal vector is obtained by evaluating the shape functions at position $x_p(t)$.

(c) Gyroscopic torque of the rifling. The angular acceleration imparted by the rifling transmits a reactive torque to the barrel, which can be modelled as a distributed moment proportional to $\dot{v}(x_p)$. This effect, weaker than (a) and (b), can be neglected in a first analysis.

(d) Projectile position. The internal kinematics $x_p(t)$ is obtained by integrating the internal-flow equation:

$$m_p\,\ddot{x}_p \;=\; p(t)\,A_b \;-\; F_{\text{frict}}(x_p,\dot{x}_p), \tag{10}$$

where A_b is the effective bore cross-section and F_{frict} the engagement resistance. The exit time t_b satisfies $x_p(t_b)=L$; for .22 LR Match in a 26" barrel, $t_b \approx 1.5$ to 1.7 ms.

3.5 Newmark–β time-integration scheme

The semi-discrete equation of the structure reads

$$[M]\{\ddot{u}(t)\} \;+\; [C]\{\dot{u}(t)\} \;+\; [K]\{u(t)\} \;=\; \{F(t)\}, \tag{11}$$

where $[C]$ is usually modelled by Rayleigh damping $[C]=\alpha_M[M]+\alpha_K[K]$ with two constants (α_M,α_K) calibrated against measured modal damping ratios ($\zeta_1 \sim 0.5\,\%$ to $1\,\%$ for a steel barrel).

The implicit Newmark–β scheme advances from step n to step $n+1$ (with Δt) by:

$$\{u_{n+1}\} = \{u_n\} + \Delta t\,\{\dot{u}_n\} + \tfrac{\Delta t^2}{2}\big((1-2\beta)\{\ddot{u}_n\} + 2\beta\,\{\ddot{u}_{n+1}\}\big), \tag{12}$$

$$\{\dot{u}_{n+1}\} = \{\dot{u}_n\} + \Delta t\,\big((1-\gamma)\{\ddot{u}_n\} + \gamma\,\{\ddot{u}_{n+1}\}\big), \tag{13}$$

where $\{\ddot{u}_{n+1}\}$ is obtained by re-injecting (12) into (11) evaluated at t_{n+1}, leading to the linear system:

$$\Big([M] + \gamma\,\Delta t\,[C] + \beta\,\Delta t^2\,[K]\Big)\,\{\ddot{u}_{n+1}\} \;=\; \{F_{n+1}\} - [C]\{\dot{u}^{\star}_n\} - [K]\{u^{\star}_n\}, \tag{14}$$

where $\{u^{\star}_n\}$ and $\{\dot{u}^{\star}_n\}$ are the predictors built from the current values. The classic pair $(\gamma,\beta)=(1/2,1/4)$ (*average constant acceleration*) is *unconditionally stable* and conserves energy with no numerical dissipation; it is favoured here to faithfully preserve the amplitude of excited modes. The time step must nevertheless resolve the highest frequency of interest: we take $\Delta t \lesssim T_{\max}/20$, where $T_{\max}$ is the period of the highest physically significant mode (typically a few kHz for a barrel, hence $\Delta t \sim 10\,\mu$s).

4 Modal analysis and sensitivity to the tuner

4.1 Eigenvalue problem

In the absence of damping and excitation, we seek harmonic solutions $\{u(t)\}=\{\phi\}\,e^{\mathrm{i}\omega t}$, which reduces (11) to a generalised eigenvalue problem:

$$\big([K]-\omega^2[M]\big)\,\{\phi\} = \mathbf{0}. \tag{15}$$

The solutions $(\omega_n^2,\{\phi_n\})$ give the natural angular frequencies ω_n and the mode shapes $\{\phi_n\}$. The frequencies in hertz are $f_n=\omega_n/(2\pi)$. For the reference barrel of the simulator (steel, $L=0.66\,$m, $D_{\text{ext}}=24\,$mm cylindrical, $D_{\text{int}}=5.6\,$mm), a 20-element FEM solution gives the following first modes:

Mode	Bare barrel	200 g tuner	400 g tuner
f_1 (Hz)	39.87	34.16	30.33
f_2 (Hz)	230.1	217.66	206.9
f_3 (Hz)	633.5	602.39	575.1
f_4 (Hz)	≈1.19 kHz	1.14 kHz	1.09 kHz
f_5 (Hz)	≈1.87 kHz	1.79 kHz	1.72 kHz

The analytical solution for the bare cantilever beam, $f_1 = \frac{1.875^2}{2\pi}\sqrt{EI/(\rho A L^4)}$, gives $f_1 \approx 40.0$ Hz, in perfect agreement with the FEM result (39.87 Hz). Adding a 200 g tuner at the muzzle drops f_1 by about 14 % (from 39.9 to 34.2 Hz); a 400 g tuner gives a 24 % reduction. This range largely covers the useful time window around $t_b \approx 2$–3 ms.

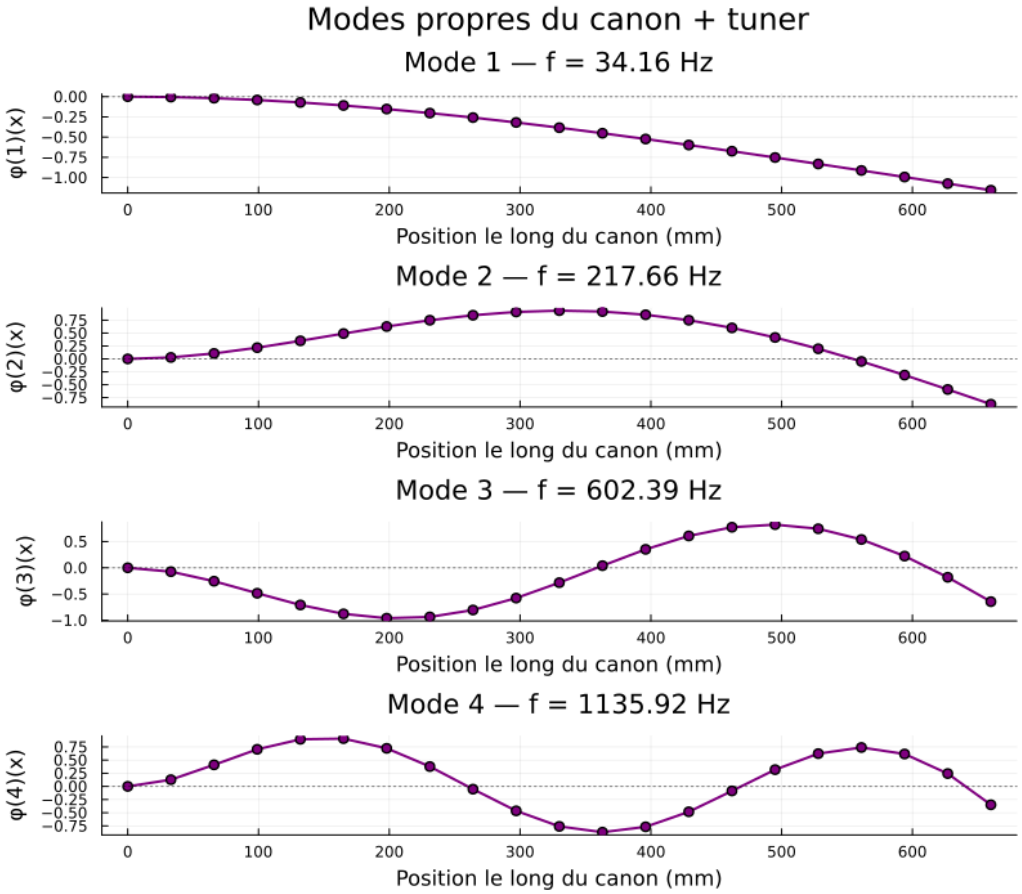

Figure 3: First four mode shapes $\phi_n(x)$ of the barrel fitted with a 200 g tuner (FEM calculation, 20 elements). Note the monotonic shape of mode 1 (spatial antinode at the muzzle), and the progressive migration of the spatial nodes of higher modes toward the muzzle, a consequence of mass concentration at $x = L$.

4.2 Sensitivity via the Rayleigh quotient

The *Rayleigh quotient* associated with mode n reads

$$\omega_n^2 \;=\; \frac{\{\phi_n\}^{\top}[K]\{\phi_n\}}{\{\phi_n\}^{\top}[M]\{\phi_n\}}. \tag{16}$$

Let $\phi_n^{(L)}$ denote the mode component at the muzzle node (in translation). A perturbation δm_t of the tuner mass modifies $[M]$ by $\delta m_t\, \phi_n^{(L)\,2}$ in the denominator, without affecting $[K]$. To first order, we obtain:

$$\boxed{\frac{\mathrm{d}\omega_n^2}{\mathrm{d}m_t} \;\approx\; -\,\omega_n^2\, \frac{\left|\phi_n^{(L)}\right|^2}{\{\phi_n\}^\top [M] \{\phi_n\}} \;\leq 0.} \tag{17}$$

Two important conclusions follow:

1. Adding mass at the muzzle *always lowers* the frequency (negative sign).
2. The reduction is more pronounced when the mode has a large amplitude at the muzzle. For the fundamental mode of a cantilever beam, $\phi_1^{(L)}$ is maximum, so f_1 drops strongly; for mode 2, the vibrational node moves closer to the muzzle, and the tuner's effect is more modest.

These properties form the basis of the tuning mechanism: by moving the position of a sliding mass (or stacking weights), the shooter continuously sweeps f_1 over a typical range of ± 15 to $\pm 30\,\%$.

4.3 Modal decomposition and transient response

By decomposing the response onto the basis of mass-normalised mode shapes, $\{u(t)\} = \sum_n q_n(t)\{\phi_n\}$, equation (11) decouples into

$$\ddot{q}_n(t) + 2\zeta_n \omega_n\, \dot{q}_n(t) + \omega_n^2\, q_n(t) \;=\; f_n(t), \quad f_n(t) = \{\phi_n\}^\top \{F(t)\}. \tag{18}$$

For an impulsive excitation (the pressure+projectile signature resembles a pulse of a few hundred microseconds), each mode begins a free oscillatory regime. The global rotational response at the muzzle is then

$$\theta(L,t) \;=\; \sum_n \phi_n^{\theta(L)}\, q_n(t), \tag{19}$$

where $\phi_n^{\theta(L)}$ is the rotation component of mode n at the muzzle node. In practice, the first mode dominates the muzzle kinematics at characteristic times $\sim t_b$; it is therefore essentially its tuning that the tuner targets.

A transient regime, not an established standing wave. A caveat is in order, one that Kolbe [7] makes the heart of his argument: it is tempting to represent "how a barrel vibrates" by the *analytic standing-wave solutions* of the beam equation. Yet these waves do *not* form during the useful window. Their phase velocity is too low for a steady standing-wave regime to establish itself over the $t_b \approx 1$–3 ms of bullet passage: at that instant the barrel is still within the *transient response* to the impulsive recoil moment, not in a settled periodic regime. This is precisely why the modal decomposition above is exploited here as a *forced transient response* (integrated step by step by Newmark-β) rather than as a superposition of modes with frozen amplitudes, and why the reasoning of Section 5.3 favours the *temporal node* (the instantaneous state of the oscillation at t_b) over the spatial node (a property of a fully established mode).

5 Muzzle kinematics and positive compensation

5.1 Travel time and muzzle angle

Let $v(x,t)$ denote the projectile velocity at position x; the exit time is

$$t_b \;=\; \int_0^L \frac{\mathrm{d}x}{v(x)}. \tag{20}$$

The effective launch angle at exit reads

$$\theta_{\mathrm{out}} \;=\; \theta(L,t_b) \;=\; \left.\frac{\partial y}{\partial x}\right|_{x=L,\,t=t_b}. \tag{21}$$

A variation $\Delta\theta_{\mathrm{out}}$ produces a vertical displacement on target (at distance D, to first order without ballistic correction):

$$\Delta h \;\approx\; D\,\Delta\theta_{\mathrm{out}}. \tag{22}$$

The underlying geometry is that of figure 1 in the introduction: what section 1 described qualitatively is here reformulated in terms of muzzle angle and on-target effect.

5.2 Coupling between velocity spread and vertical dispersion

A variation Δv_0 of the muzzle velocity induces two cumulative effects:

1. *Additional ballistic drop.* At distance D, for a flat trajectory, the drop below line of sight is $h_{\mathrm{bal}}(v_0) \simeq gD^2/(2v_0^2)$, hence

$$\frac{\partial h_{\mathrm{bal}}}{\partial v_0} \;\simeq\; -\frac{gD^2}{v_0^3} \;<\; 0. \tag{23}$$

   Numerically, at $D = 50\,\mathrm{m}$ and $v_0 \approx 308\,\mathrm{m/s}$ (1010 ft/s, .22 LR Match), $\partial h_{\mathrm{bal}}/\partial v_0 \approx -0.84\,\mathrm{mm/(m/s)}$, i.e. roughly -0.016 MOA per ft/s; this is also the number computed by Kolbe [5] using a trajectory solver.

2. *Exit-time shift.* The internal kinematics couples t_b and v_0: in the limit, $t_b \propto 1/v_0$ gives $\partial t_b/\partial v_0 = -t_b/v_0$, but the actual dependence is stronger because a more energetic charge raises the pressure *throughout* the bore and shortens t_b more than a simple kinematic ratio. We therefore write

$$\tau_v \;\equiv\; -\frac{\partial t_b}{\partial v_0} \;>\; 0, \tag{24}$$

   a quantity directly measurable using a chronograph coupled to a muzzle-exit sensor. Kolbe reports [5], for Eley Tenex in a 26" barrel,

$$\tau_v \;\approx\; \frac{1\ \mathrm{ms}}{375\ \mathrm{ft/s}} \;=\; \frac{1\ \mathrm{ms}}{114\ \mathrm{m/s}} \;\approx\; 8.8\ \mu\mathrm{s}\,/\,(\mathrm{m/s}), \tag{25}$$

   and argues that this value is, to within $\pm 10\,\%$, a constant for rimfire barrels longer than 6 inches.

The positive-compensation condition requires the two contributions to cancel on target:

$$\boxed{\left.\frac{\mathrm{d}\theta_{\mathrm{out}}}{\mathrm{d}t}\right|_{t_b} \cdot \Delta t_b \;+\; \frac{1}{D}\frac{\partial h_{\mathrm{bal}}}{\partial v_0}\Delta v_0 \;=\; 0.} \tag{26}$$

Substituting $\Delta t_b = -\tau_v\,\Delta v_0$ and (23), we obtain the *optimal angular velocity* at the muzzle at the moment of exit:

$$\dot{\theta}^{\star}_{\mathrm{out}} \;=\; \frac{1}{D\,\tau_v}\,\frac{\partial h_{\mathrm{bal}}}{\partial v_0} \;=\; -\,\frac{g\,D}{v_0^3\,\tau_v}. \tag{27}$$

The negative signs of $\partial h_{bal}/\partial v_0$ and $\partial t_b/\partial v_0$ combine to make $\dot{\theta}^{\star}_{out}$ positive: the muzzle must therefore be rising ($\dot{\theta} > 0$) at the moment of shot release. Numerically, with $D = 50\,\mathrm{m}$, $v_0 = 308\,\mathrm{m/s}$ and $\tau_v = 8.8\,\mu\mathrm{s/(m/s)}$:

$$\dot{\theta}^{\star}_{\mathrm{out}} \;\approx\; 1.9\ \mathrm{mrad/ms} \;\approx\; 6.6\ \mathrm{MOA/ms},$$

to be compared with the 6.0 MOA/ms experimentally measured by Kolbe (the $\sim 10\,\%$ discrepancy is explained by the non-flatness of the trajectory at 50 m and the approximations on τ_v).

5.3 Spatial node *vs* temporal node: a semantic clarification

The vocabulary of *node* and *antinode*, inherited from the acoustics of standing waves, often causes confusion when applied to shooting. Two physically distinct meanings coexist:

Spatial node/antinode — special points of the *mode shape* $\phi_n(x)$ along the barrel: a *spatial node* is an $x^\star$ such that $\phi_n(x^\star) = 0$ (zero transverse displacement); a *spatial antinode* is an $x^\star$ where $|\phi_n|$ reaches a local maximum. For the fundamental mode of a cantilever beam, the shape is monotonically increasing from 0 (clamped end) to $\phi_1(L)$ (muzzle). **The muzzle is therefore, by construction, a spatial antinode of mode 1.** No choice of tuner moves this property: the muzzle remains where the bullet exits, at $x = L$.

Higher modes ($n \geq 2$), on the other hand, exhibit spatial nodes *inside* the barrel. Placing the tuner precisely at a spatial node of mode n makes that mode insensitive to the added mass (cf. generalisation of (17) to a mass positioned away from $x = L$). This is the trick of so-called *harmonically-balanced* tuners: f_1 can be adjusted without disturbing f_2 or f_3, which makes the adjustment more monotonic and reproducible.

Temporal node/antinode — special points of the *in-time* oscillation of the muzzle angle $\theta(L, t)$: a *temporal node* is an instant $t^\star$ where $\theta(L, t^\star) = 0$ (zero crossing); a *temporal antinode* is an instant where $|\theta(L, t)|$ reaches a maximum (i.e. $\dot{\theta}(L, t^\star) = 0$). For a nearly sinusoidal mode 1, these two types of instants alternate at a quarter period.

The criterion (27) then translates unambiguously:

Exit instant t_b	$\theta(L, t_b)$	$\dot{\theta}(L, t_b)$
Temporal antinode	$\pm\Theta_1$ (max)	0
Temporal node	0	$\pm\Theta_1\,\omega_1$ (max)

Positive compensation requires exit in the vicinity of an *ascending temporal node*, where $\theta = 0$ and $\dot{\theta} > 0$ is at its maximum. Exiting at the peak of the oscillation (temporal antinode) is, on the contrary, the *worst* case: not only does $\dot{\theta} = 0$ wipe out any compensation, but one also fires with a maximum static angular offset that shifts the mean point of impact.

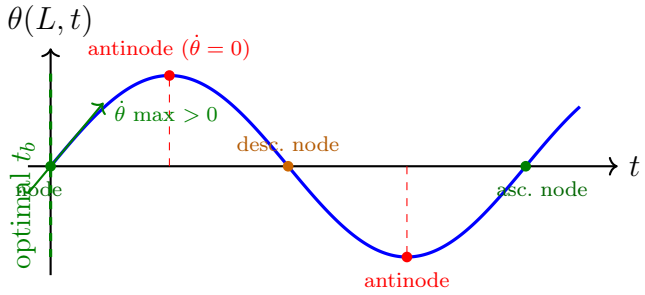

Figure 4: Temporal node vs antinode distinction on the muzzle angle $\theta(L,t)$. Positive compensation requires t_b to fall in the vicinity of an *ascending temporal node* (green point at $t = 0$ and $t = T_1$), where $\theta = 0$ but $\dot{\theta}$ is maximum and positive. Exiting at a temporal antinode (red points, $\dot{\theta} = 0$) cancels the compensation.

What Kolbe [5, 6] calls the "upward swing of the vibration at the muzzle" corresponds precisely to this *ascending temporal node*. In the competitor jargon (*ladder* or *OCW* [9] method), the "node" of tuning refers more loosely to a zone of *robustness* of grouping, i.e. a plateau around which a small shift of t_b does not degrade the group. In the strict sense of vibration mechanics, this plateau is precisely the window around an ascending temporal node — where $\ddot{\theta}(L,t_b)$ is close to zero and $\dot{\theta}(L,t_b)$ hovers near its extremal value, which makes the tuning weakly sensitive to fluctuations of t_b.

5.4 Experimental confirmation (Kolbe, 2015)

Kolbe [6] directly verified the criterion (27) on an instrumented test bench measuring the muzzle angle optically (crossed polariser) with a photo-detector gate locating the exact exit instant. On a 26" Border barrel, .22 LR calibre, Eley EPS Tenex ammunition, two configurations are compared:

Configuration	measured $\dot{\theta}(L,t_b)$	On-target groups
Bare barrel	-9.4 MOA/ms (muzzle dropping)	pronounced *vertical* string
Barrel + 200 g tuner	$+6.0$ MOA/ms (muzzle rising)	*round* groups

The value $+6.0$ MOA/ms coincides with criterion (27) for 50 m and the ammunition used. The near-complete elimination of vertical stringing experimentally confirms that the criterion is not only necessary (sign) but also sufficient (magnitude) when higher-order modes remain weakly excited.

In particular, Kolbe notes that the *vertical translation velocity* $\dot{y}(L,t_b)$ of the muzzle contributes negligibly to the on-target dispersion compared to $\dot{\theta}(L,t_b)$: it is indeed the muzzle's *rotation*, not its translation, that determines the effective launch angle. This observation justifies *a posteriori* the DOF split (translation + rotation) of the FEM model, and orients the control toward extracting the rotational component at the terminal node.

5.5 Validation by FEM + Newmark-β simulation

The `Julia` simulator accompanying this document (`simulation.jl`) implements the full formalism: FEM assembly, clamping, tuner, internal ballistics (exponential model calibrated on t_b and v_{muzzle}), excitation by the breech recoil moment $M(t) = p(t)\, A_{\text{bore}}\, h_{\text{offset}}$, moving projectile load, Rayleigh damping and Newmark-β scheme. The lever arm h_{offset} is automatically calibrated to reproduce the vibration envelope measured by Kolbe (~ 10 MOA/ms peak).

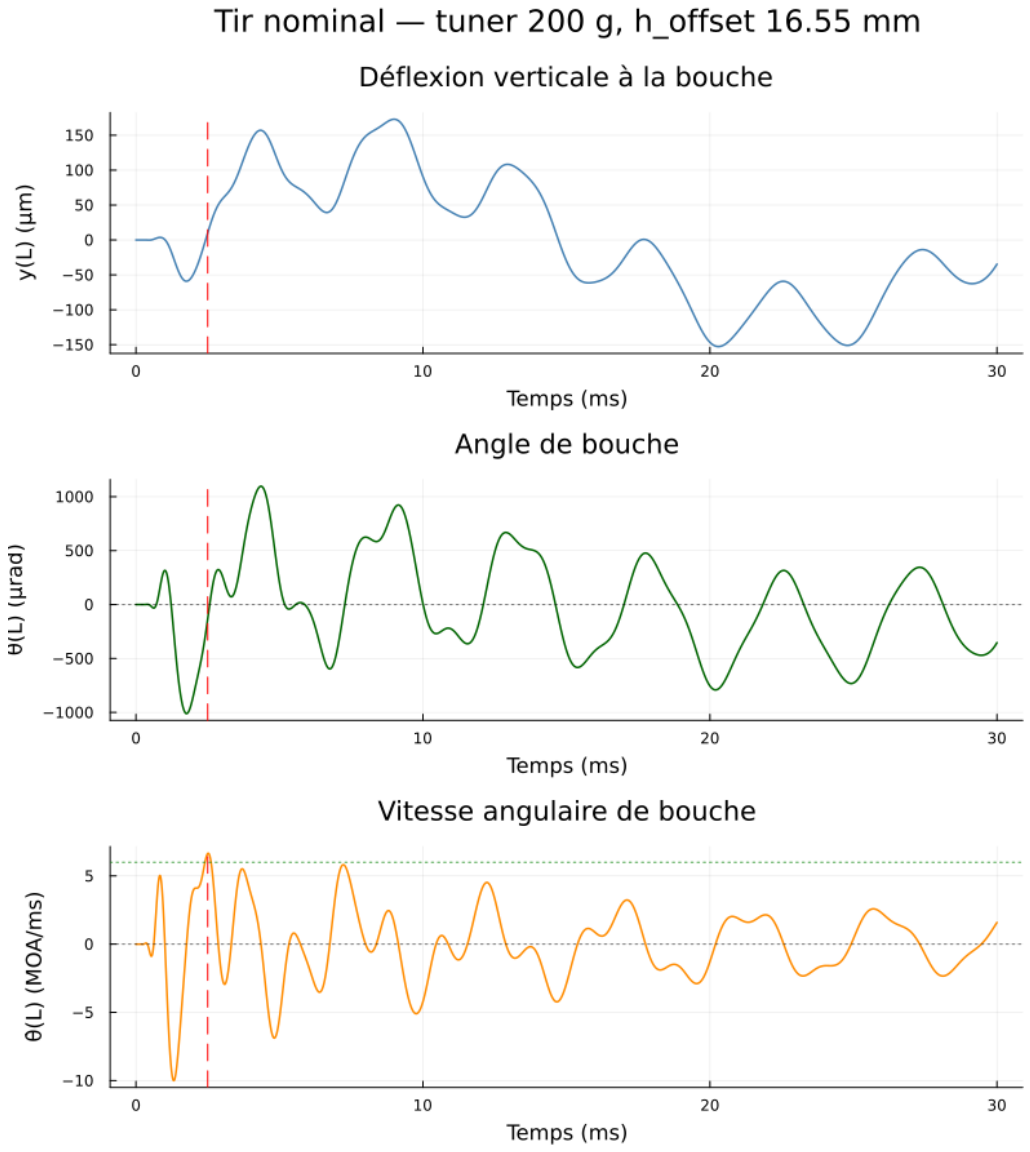

Figure 5: Simulated transient response for the nominal configuration (200 g tuner, $h_{\text{offset}} = 16.5$ mm). From top to bottom: deflection $y(L,t)$, muzzle angle $\theta(L,t)$, and angular velocity $\dot{\theta}(L,t)$. The red dashed line marks $t_b = 2.5$ ms; the green dotted line in the bottom panel indicates the Kolbe target (6 MOA/ms). The value computed at t_b is +6.64 MOA/ms, agreeing to within $\sim 10\,\%$ with the measurement.

These plots illustrate a distinction essential for the shooter: the tuner acts *primarily on the mean point of impact* (via $\theta(L, t_b)$) and *secondarily on the vertical dispersion* (via $\dot{\theta}(L, t_b)$). When $t_b \ll T_1$, the optimality window in $\dot{\theta}$ is wide and flat; the tuner adjustment

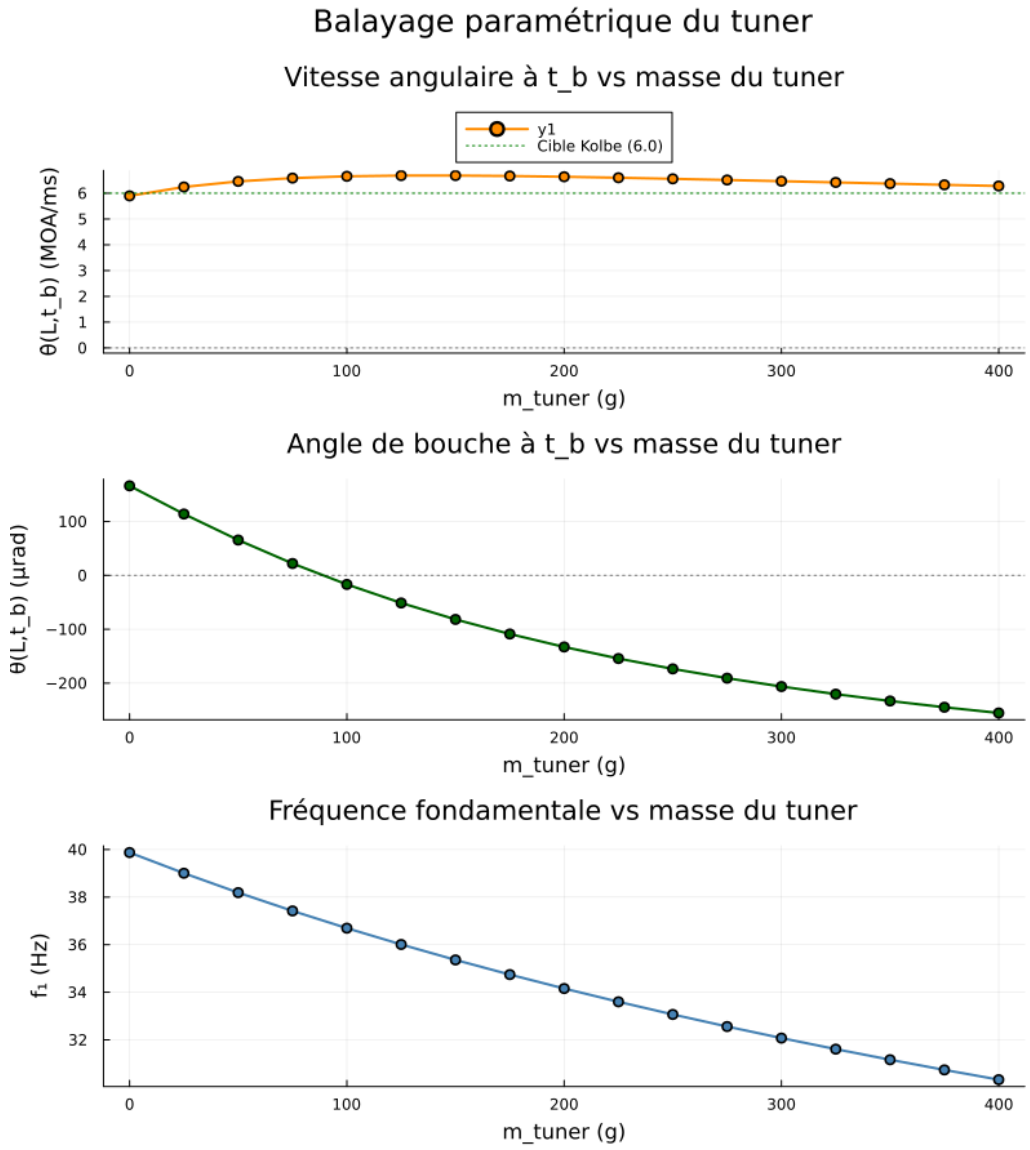

Figure 6: Parameter sweep on the tuner mass $m_t \in [0, 400]$ g (other parameters fixed). From top to bottom: (i) $\dot{\theta}(L, t_b)$ varies little (5.9 to 6.7 MOA/ms) because $t_b/T_1 \approx 0.085$ remains in the initial rising quarter cycle; (ii) $\theta(L, t_b)$, on the contrary, varies strongly and monotonically (+166 to −255 µrad), reflecting a shift of the mean point of impact; (iii) f_1 decreases monotonically from 39.9 to 30.3 Hz (relation predicted by the Rayleigh quotient, equation (17)).

then mainly serves to compensate for the velocity spread, while the sight adjustment takes care of the POI shift.

6 Practical conclusions for the shooter

The preceding formalism, validated numerically by the finite-element simulation, leads to several exploitable conclusions.

1. Effect of a muzzle mass. Adding a mass at the muzzle *lowers* the fundamental frequency (cf. (17)). For the reference barrel, the adjustment range of a 100–400 g tuner covers an f_1 variation of the order of 8 to 24 % (39.9 Hz $\to$ 30.3 Hz). The equivalent temporal shift in the vibration cycle is of the order of a fraction of a millisecond, which suffices to sweep the entire optimality window in which $t_b \approx 2$–3 ms must be positioned.

2. Direction of adjustment. Extending the effective tuner position (screwing it outward) increases J_t and the lever arm, which amplifies the mass effect and lowers f_1. This is the action that "slows down" the muzzle kinematics and delays the zero crossing of $\theta(L,t)$: useful for slower ammunition (delayed exit t_b).

3. Sensitivity to ammunition. Any change of lot or brand modifies $\bar{v}$ and therefore t_b. The optimality window ($\dot{\theta}_{\text{out}}$ near $\dot{\theta}^{\star}_{\text{out}}$) is narrow: a 0.1 ms shift on t_b may represent a non-negligible fraction of the period $T_1 = 2\pi/\omega_1$. Any new lot must therefore be the subject of a systematic retuning at the tuner notch (*ladder tune* or *Audette* method).

4. Physical limits. The tuner does not remove the intrinsic dispersion of the ammunition: it converts a vertical dispersion into a genuinely tighter group only if (26) is satisfied to within a few MOA/ms. The horizontal dispersion, independent of the (Δv_0, θ_{out}) pair, is not compensated. The expected on-target gain therefore remains bounded by the other error sources (wind, bullet imbalance, parallax, sight).

5. Robustness to higher modes. Modes 2 and 3, of significantly higher frequencies (cf. the previous table), produce a fast oscillation superposed on $\theta(L,t)$. If they are poorly damped and significantly excited, they create a residual variability (*flyers*) even after tuning. A muzzle mass distinct from an integer harmonic of mode 1 (anti-resonance) helps filter them out, which motivates the "adjustable" double-ring designs.

6. Range of validity: centerfire *vs* rimfire. A caveat of intellectual honesty, stated by Kolbe himself [7], deserves to be reported. The *principle* of positive compensation (Sections 1 and 5) is general and was first established for rimfire. The *impulsive recoil-moment excitation model* adopted here (and in Kolbe's simulator), however, is chiefly relevant to *centerfire* calibres: there the pressure–time curve is long ($\sim$ 1 ms, peak $\sim$ 350 MPa $\approx$ 50,000 psi, .308 Win-like profile) and the recoil high, so that the recoil moment does dominate the onset of vibration. For the *.22 LR*, the pressure pulse is so brief that, according to Kolbe, the recoil moment alone reproduces the observed vibrations poorly: *other* excitation sources (rifling engagement, the moving projectile's weight effect, assembly play) take a comparable share. Our model captures them partially — this is the very purpose of contributions (b) and (c) of Section 3.4, absent from Kolbe's original simulator — but the rimfire numbers given in this document should be read as *calibrated orders of magnitude*, not absolute predictions. Direct experimental validation (Section 5.5) remains the reference for rimfire.

Bibliography

References

[1] S. S. Rao, *Mechanical Vibrations*, Pearson, 2017.

[2] L. Meirovitch, *Elements of Vibration Analysis*, McGraw-Hill, 1986.

[3] K.-J. Bathe, *Finite Element Procedures*, 2nd ed., Prentice Hall, 2014.

[4] D. Carlucci and S. Jacobson, *Ballistics: Theory and Design of Guns and Ammunition*, 3rd ed., CRC Press, 2018.

[5] G. Kolbe, *Using barrel vibrations to tune a barrel — The Vibrations of a Barrel Tuned for Positive Compensation*, Border Barrels, 2015.

[6] G. Kolbe, *The Vibrations of a Barrel Tuned for Positive Compensation* (online article, updated 18 November 2015), `http://www.geoffrey-kolbe.com/articles/rimfire_accuracy/tuning_a_barrel.htm`.

[7] G. Kolbe, *Barrel Vibrations Simulator* ("lumped parameter" finite-element model and modelling notes, online, accessed June 2026), `http://www.geoffrey-kolbe.com/articles/rimfire_accuracy/barrel_vibrations.htm`.

[8] A. Mallock, *Vibrations of Rifle Barrels*, Proceedings of the Royal Society, Vol. 68, p. 327, 1901. `https://www.tireur.org/articles/Mall01.pdf`.

[9] C. Audette, *The Optimum Charge Weight (OCW) Method*, *Precision Shooting Magazine*, 2005–2010.

[10] N. M. Newmark, *A Method of Computation for Structural Dynamics*, ASCE Journal of the Engineering Mechanics Division, 85(3), pp. 67–94, 1959.